Research Article | Vol. 27, No. 7 | 1 Apr 2019 | OPTICS EXPRESS 10296
Optics EXPRESS

100 kW peak power external cavity diamond Raman laser at 2.52 μm

GIORGOS DEMETRIOU,* ALAN J. KEMP, AND VASILI SAVITSKI

Institute of Photonics, Department of Physics, SUPA, University of Strathclyde, 99 George Street, Glasgow G1 1RD, UK
**giorgos.demetriou@strath.ac.uk*

Abstract: We report an external cavity diamond Raman laser operating at 2.52 μm, pumped by a 1.89 μm Tm:LiYF4 (YLF) laser. The maximum pulse energy at 2.52 μm is 1.67 mJ for 4.4 mJ of pump, yielding a conversion efficiency of 38%. The best slope efficiency is ~60% and the Raman pulse duration is between 11 and 15 ns for ~33 ns pump pulse duration. The peak power at 2.52 μm is >100 kW. This demonstration of a Thulium laser pumped diamond Raman laser paves the way for accessing the industrially important wavelength region of ~2.5 μm.

1. Introduction

Lasers operating in the short-wave infrared (SWIR or IR-B: 1.4-3 μm [1]) region of the electromagnetic spectrum are important for applications including sensing [2], free space communications [3] and materials processing [4]. However, SWIR solid-state laser technology, especially in the region of 2-3 μm, has yet to fully mature, relying on a limited range of doped-crystalline [2,5,6], Raman [7–11], and fiber lasers [12,13]. As a result, there is a continuing interest in new means to access this important wavelength region, either directly or by wavelength conversion.

A major driver for this is that the absorption of many clear (transparent in visible) plastics used in medicine and aerospace is significant at wavelengths longer than ~2.45 μm [4,14]. A high power laser operating in this region would enable processing of such plastics without prior modification (e.g. Butt welding [4]). Diamond Raman lasers (DRL) pumped by Thulium lasers (~1.9 μm) are an appealing solution to this problem, producing a 1st Stokes output at ~2.55 μm based on wavelength conversion of a mature laser technology.

Moreover, the high Raman gain coefficient [15,16], unrivalled thermal conductivity [17], and high damage threshold [18,19] of diamond make it an excellent candidate for high power applications. This crystal also has a very broad transmission range extending from ultraviolet to THz [20]. There is, however, a reduction in transmission between ~2.5 and ~6.5 μm caused by multiphonon absorption [20]. This feature limited the efficiency of a diamond Raman laser operating in the 3.38-3.80 μm wavelength region to 15% [21].

In this work, a Tm:YLF laser operating at ~1.89 μm was used to pump a DRL at ~2.52 μm. This wavelength is located at the edge of multiphonon absorption in diamond and the results reported here demonstrate the feasibility of efficient Raman oscillation in this spectral region with a longer term view of power scaling for implementation in industrial applications, particularly clear plastics processing. As a next step in power scaling the DRL, it is planned to use a high power Tm fiber laser as a pump source. The majority of Tm fiber lasers tend to operate more efficiently at wavelengths longer than ~1.91 μm due to the more efficient cross-relaxation processes at these wavelengths [22]. This increases the Tm fiber laser wall plug efficiency. Pump wavelengths longer than ~1.91 μm would result in the DRL oscillating at wavelengths > 2.56 μm. However, multiphonon absorption in diamond increases sharply above ~2.55 μm and therefore efficient Raman oscillation in this region would be

#359336 https://doi.org/10.1364/OE.27.010296
Journal © 2019 Received 1 Feb 2019; revised 28 Feb 2019; accepted 13 Mar 2019; published 28 Mar 2019

Optics EXPRESS

compromised. As a result, the choice of output wavelength for a Tm fiber pumped DRL will be a compromise between the efficient operation of the Tm fiber pump laser and the multiphonon absorption in diamond at the Raman wavelength, which is crucial for the efficiency of the Raman laser. In addition to being a feasibility study for future fiber laser pumping, this work also investigates the effect multiphonon absorption has on the DRL performance, which will subsequently define the long wavelength limit for the Tm fiber pump laser and the overall wall plug efficiency of the "Tm pumped-DRL" system.

2. Experimental setup

The Tm:YLF pump laser (Fig. 1) consisted of a 24 mm long, 2 at.% Tm:YLF crystal (with no anti-reflection (AR) coatings) held in a water-cooled brass mount and placed in a 145 mm long laser cavity. The Tm:YLF was pumped by a 795 nm diode laser and q-switched using a water-cooled acousto-optic modulator (AOM). A 1 mm thick birefringent filter (BRF) was inserted at Brewster's angle to control the output wavelength. No reasonable tunability was achieved due to the large thickness of the BRF [23]. The output wavelength was centered at ~1888 nm; however, it drifted over ~5 nm (from 1886 to 1891 nm), we believe due to the unstablized temperature and humidity of the lab. Without the BRF in the cavity, the output wavelength shifted to ~1.91 µm. The linewidth of the Tm:YLF laser, after inserting a 1 mm thick quartz etalon in the cavity, was between 0.37 and 0.66 nm. The maximum pulse energy was ~5.5 mJ at 5 Hz repetition rate and the pulse duration, measured with a 10 GHz InGaAs detector, was ~33 ns. This equates to a peak power of ~0.17 MW. The output was horizontally polarized.

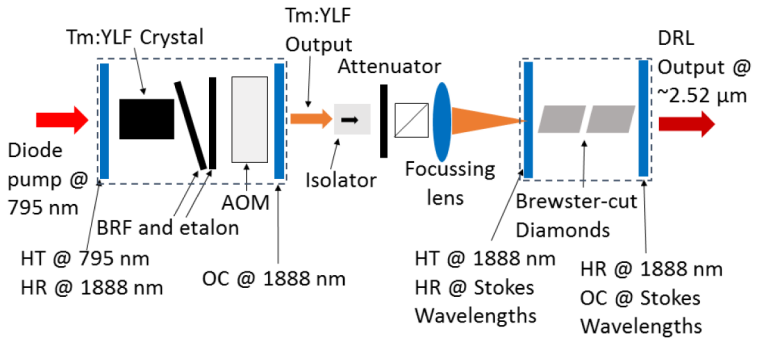

Fig. 1. Layout of the experimental setup, including both the Tm:YLF pump laser and diamond Raman laser.

The Tm:YLF laser was used to pump a DRL at ~2.52 µm (Fig. 1). Two Brewster-cut diamonds with lengths of 4- and 5.6 mm were used, giving an overall diamond length of 9.6 mm. The diamonds had low-nitrogen content, low birefringence and where grown via chemical vapor deposition by Element Six (UK) Ltd. Both crystals were cut for pump propagation along a <110> direction. The pump polarization was parallel to a <110> axis of the 5.6 mm crystal and a <111> axis of the 4 mm long diamond. Here it should be noted that due to the unavailability of a longer crystal, two different diamond crystals needed to be used in order to reach Raman threshold and the two crystals described above were the only two available.

These diamonds were separated by a small air-gap and placed within a 12.5 mm long cavity. A curved mirror (50 mm radius of curvature, highly transmissive (HT) for ~1.9 µm and highly reflective (HR) for ~2.55 µm) was used as input coupler, whereas two different plane mirrors were used as output couplers (OC). The 1st OC had 90% reflectivity at the pump wavelength and 93.5% reflectivity (i.e. 6.5% output coupling) at the Stokes wavelength, whereas the 2nd OC had 80% reflectivity (20% output coupling) at both pump and Stokes wavelengths.

Optics EXPRESS

The output of the Tm:YLF laser was focused into the diamonds (Fig. 1) using two different CaF_2 lenses, both AR-coated for ~1.9 µm, with focal lengths of 75- and 100 mm, yielding beam radii at focus of 52.5- and 70 µm, in free space, respectively. The beam quality of the pump was measured with the knife-edge method to be 1.2. The corresponding confocal parameters were ~7.8 mm and ~13.8 mm respectively. The change in the beam dimensions due to the Brewster-cut nature of the diamonds was taken into account in all the subsequent calculations in this work. The intracavity Raman mode radii were calculated with the ABCD matrix method to be ~137x304 µm, varying within ± 5 µm along the length of the diamonds.

3. Results and discussion

The energy transfer characteristics of the DRL for both focusing lenses and both OCs are presented in Fig. 2. The best slope efficiency was 60 ± 4% for the 75 mm lens with 20% output coupling, whereas the worst slope efficiency was 36 ± 3%, for the case of the 75 mm lens and 6.5% output coupling. The slope efficiencies in the case of the 100 mm lens were 44 ± 4% and 46 ± 4% for 6.5% and 20% output coupling respectively. The maximum output pulse energy was 1.67 mJ for 4.4 mJ of pump, for the case of the 100 mm lens and 20% output coupling, yielding a maximum conversion efficiency of 38%. It should be noted that with a 6.5 mm long AR-coated cuboid diamond being placed in the cavity instead of the pair of Brewster-cut diamonds, damage of the coatings was observed at a pump pulse energy of ~0.5 mJ with no Raman oscillation.

Raman laser operation is achieved at lower incident peak intensities (top axes of Figs. 2(a), 2(b) and Fig. 2(c)) with the 100 mm lens. The DRL operates from ~0.17 to ~0.37 GW/cm^2, whereas for the 75 mm lens it operates from ~0.28 to ~0.68 GW/cm^2. This is attributed to the pump confocal parameter of the 75 mm lens (7.8 mm) being smaller than the overall diamond length (9.6 mm). This limits the extent to which tighter focusing can be used to increase DRL efficiency.

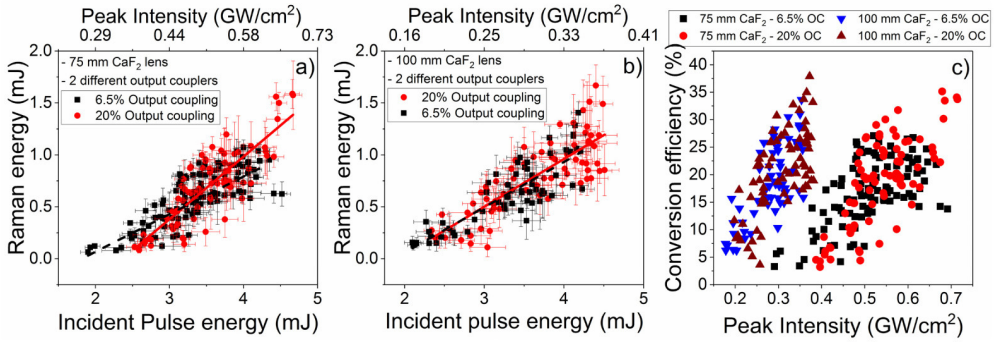

Fig. 2. Energy transfer characteristics for both output coupling levels used for the DRL with (a) 75 mm lens and (b) 100 mm lens. (c) – the conversion efficiency from pump to Raman energy as a function of the incident peak intensity for both lenses and output coupling levels used. Solid and dashed lines in (a) and (b) are the results of linear fits to the experimental data for the 20% (solid line) and 6.5% (dashed line) output mirrors.

The large error bars and data spread on Fig. 2 are indicative of a lack of pulse-to-pulse stability. The Raman and pump pulse energies were not measured simultaneously, therefore the instabilities in the pump pulse energies (horizontal error bars in Figs. 2(a) and 2(b)) may have resulted in significant jitter in the Raman pulse energies. Additional factors that are likely to play a role in the DRL output pulse energy instabilities are threefold. First, the longitudinal mode-beating in the Tm:YLF pump laser. This was observed (with a fast detector – oscilloscope combination, 10 and 13 GHz bandwidth respectively) in parallel to the DRL operation. The mode-beating in the pump laser resulted in more unstable performance of the DRL. Second, the DRL is operating relatively close to threshold with the highest pump pulse

Optics EXPRESS

energies being less than two times the threshold energies. This will exacerbate the effect of variations in pump pulse energy. Third, the Raman linewidth of CVD diamond was measured to be 1.5 cm^{-1} [24,25] (0.54 nm at a wavelength of 1888 nm). Therefore, the pump laser linewidth, which varies between 0.37 and 0.66 nm, will lead to pulse-to-pulse variation in Raman gain since pump linewidths larger than the Raman linewidth lead to a concomitant reduction in gain [16,26].

Due to this high jitter in the Raman pulse energies, it was challenging to measure the M^2 factor of the Raman laser beam quality with sufficient precision using the knife-edge method (the only method available to us at the time of experiments). It is likely, however, that the Raman beam quality was no worse than that of the pump (M^2 = 1.2), similar to what was observed in [21].

Temporal pulse profiles for DRL output pulse energies of ~0.3 and ~1 mJ, are shown in Fig. 3. These include traces of the incident pump, the depleted pump after one pass and the Stokes oscillation. In all cases, the 75 mm lens and 20% output coupling were used. Pulse traces from other focusing lens - output coupling combinations were similar. For a ~33 ns pump pulse duration, the Stokes pulse durations were always in the range of 11-15 ns. This resulted in peak powers greater than 100 kW. The residual pump traces were calibrated against the leading edge of the incident pump pulse profile and they show a reduction in instantaneous power once Raman threshold has been reached, before maintaining a relatively stable power for the rest of the Stokes pulse duration. At DRL output pulse energies above 1 mJ, very strong depletion of the pump is observed (Fig. 3(b)), indicating efficient conversion to Stokes radiation.

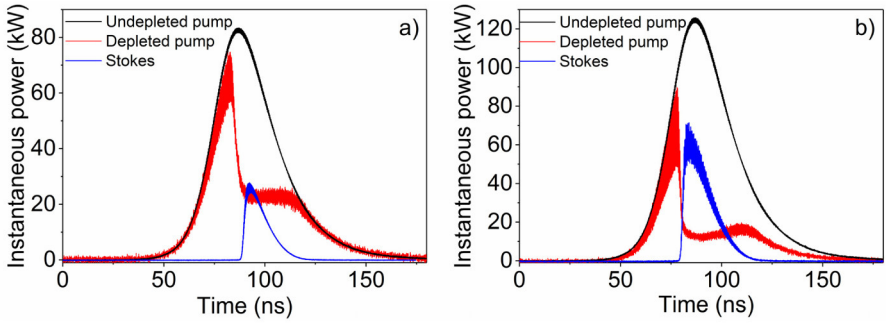

Fig. 3. Temporal pulse profiles for incident pump, single-pass depleted pump and Stokes oscillation for (a) ~0.3 mJ DRL output pulse energy and (b) ~1 mJ DRL output pulse energy.

The spectra for the Tm:YLF pump and diamond Raman lasers collected at Raman output pulse energy of ~0.5 mJ are presented in Fig. 4. These were collected with a Spectral Products CM110 monochromator with a 600 Grv/mm grating and 20 μm slits (resolution of 0.11 nm at 1890 nm and 0.14 nm at 2525 nm). For each laser (Tm:YLF pump and DRL), two cases are presented to illustrate the effect the changes in the pump spectrum have on the Raman output. Here it should be noted that the spectra for the Tm:YLF laser and the DRL were collected in two separate experimental runs. As a result, the spectrum labelled “Tm:YLF 1” is not directly correlated to the spectrum labeled “DRL 1”, and similarly for “Tm:YLF 2” and “DRL 2”. Rather, two spectra were selected for each laser to illustrate that the wavelength drift in the Tm:YLF laser results in a proportional drift in the DRL wavelength. The FWHM linewidths of the pump spectra were measured to be between 0.37 and 0.66 nm. An accurate measurement of the DRL linewidth was difficult due to the ‘tail’ feature on the short-wavelength side. It takes several minutes to collect a Raman spectrum at the laser pulse repetition rate of 5 Hz. Therefore, this tail might just represent statistics of the spectral distribution of the output DRL wavelength due to instabilities in the output spectral characteristics.

Optics EXPRESS

The multiphonon absorption spectrum in similar low-loss diamond was measured with an FTIR spectrometer (Cary 630) and is presented in Fig. 5. The output wavelength of the DRL presented in this work (~2.52 μm) lies at the onset of this multiphonon absorption. The absorption coefficient of diamond at this wavelength was ~0.11 cm^{-1}. This yields ~19% round trip intracavity losses for our diamonds (total length of 9.6 mm). These high intrinsic losses limit the conversion efficiency of the DRL.

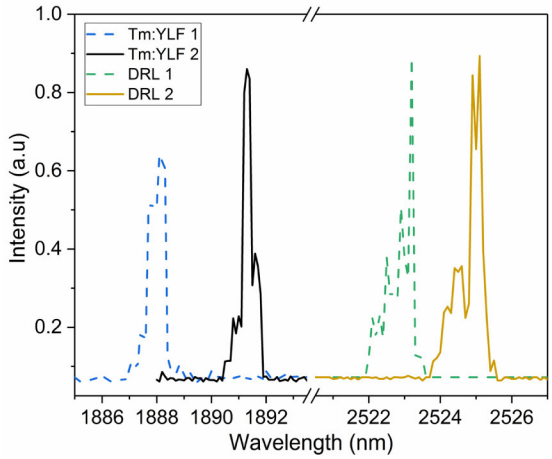

Fig. 4. Time averaged spectra of Tm:YLF pump and DRL collected with a monochromator.

Pumping at longer wavelengths, which would shift the output of the DRL deeper into the multiphonon absorption region, was investigated by rotating the BRF in the Tm:YLF cavity from Brewster's angle to normal incidence. This shifted the pump wavelength to ~1.91 μm (from ~1.89 μm) which would correspond to a 1st Stokes Raman wavelength in diamond of ~2.56 μm. Both the output wavelength of the DRL presented in this work (2.52 μm) and the expected wavelength of 2.56 μm when pumping at 1.91 μm are illustrated in the inset of Fig. 5.

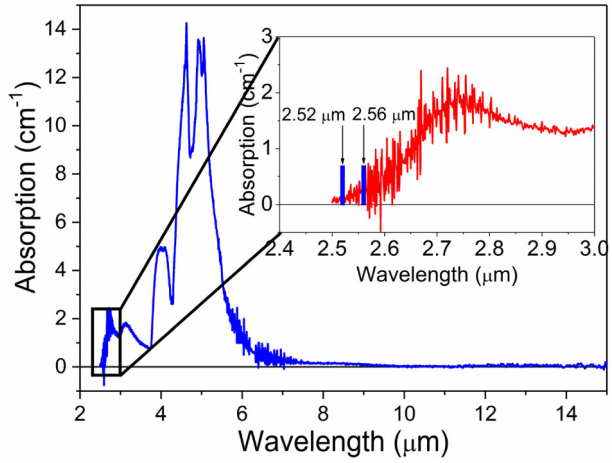

Fig. 5. Absorption coefficient of diamond from 2.5 to 15 μm measured by FTIR. Inset shows zoomed in view of the absorption coefficient in the vicinity of 2.5 to 3 μm.

The DRL was pumped at 1.91 μm with all the other parameters of the Tm:YLF laser kept the same as before except for the pulse duration which was ~40 ns rather than ~33 ns (pulse duration at 1.89 μm). Even at the highest available pump pulse energies (~4.5 mJ), which

Optics EXPRESS

correspond to peak intensities of ~0.54- and ~0.31 GW/cm^2 for the 75- and 100 mm lens respectively, no lasing action was observed in the DRL at this pump wavelength. This is attributed to the higher multiphonon absorption coefficient of diamond at 2.56 μm, which is 0.26 cm^{-1}. This value is more than double the absorption coefficient at 2.52 μm (0.11 cm^{-1}) and yields round trip losses of ~39% for the DRL.

The Raman laser threshold is reached when the round-trip steady-state Raman gain exceeds the round-trip resonator losses [27]:

$$R_1 R_2 \exp\left(2 g_R I_P l - 2\alpha l\right) \geq 1 \quad (1)$$

where R_1 and R_2 are the reflectivities of the input and output mirrors at the Stokes wavelength, g_R is the effective Raman gain coefficient at the pump wavelength, I_P is the pump peak intensity at the threshold, α is the diamond absorption coefficient at the Raman laser wavelength, and l is the length of the Raman crystal.

Using Eq. (1), an effective Raman gain coefficient [28,29] (g_{eff} in Table 1) was calculated, for the case of 1.89 μm pumping, for all focusing lens – output coupling combinations using the experimental threshold peak intensities from Figs. 2(a) and 2(b) ($I_{th–1.89μm}$ in Table 1), and an absorption coefficient in diamond of 0.11 cm^{-1} at 2.52 μm.

Effective Raman gain coefficients [28,29] are associated with the specific laser system and are lower in value than material Raman gain coefficients, due to a Raman gain reduction factor, which is a product of spatial (or transverse) and spectral overlap factors of the pump and Raman emission [28,29]. Differences in spatial overlap can explain variations in the effective Raman gain coefficients for different pump focusing lenses: this Raman gain reduction factor is lower in the case of the 100 mm lens (since for this lens the pump Rayleigh range is longer than the length of the crystals and therefore allows for better mode-matching between the pump and Raman beams in the diamonds) in comparison with the 75 mm lens (where the pump Rayleigh range is shorter than the length of the crystals). This explains why the calculated effective Raman gain was systematically higher in the case of a 100 mm lens in comparison with a 75 mm lens (see Table 1). At the same time, effective Raman gain coefficients for each focusing lens calculated for two different reflectivities of the output couplers (93.5 and 80%), are, within the experimental errors, roughly the same, indicating that spatial overlap functions are similar for different output couplers.

The Raman gain coefficient for diamond of 3.80 ± 0.35 cm/GW at a pump wavelength of 1.864 μm was measured in [30]. This is higher than the estimated effective Raman gain, mainly due to already mentioned spatial and spectral overlap factors. Spectral overlap factor takes into account reduction in the Raman gain due to broad linewidth of the pump emission in comparison with the Raman linewidth [28].

Table 1. Effective Raman gain coefficient and threshold peak intensity

Lens, mm	OC, %	R_1	R_2	$I_{th\ -\ 1.89\ μm}$, GW/cm^2	g_{eff}, cm/GW	$I_{th\ -\ 1.91\ μm}$, GW/cm^2
75	6.5	1	0.935	0.32 ± 0.04	0.45 ± 0.06	0.65 ± 0.09
	20	1	0.8	0.40 ± 0.04	0.56 ± 0.05	0.67 ± 0.06
100	6.5	1	0.935	0.20 ± 0.03	0.72 ± 0.10	0.41 ± 0.06
	20	1	0.8	0.22 ± 0.03	1.04 ± 0.14	0.36 ± 0.05

Assuming the same effective Raman gain coefficient at the pump wavelength of 1.91 μm and an absorption coefficient of 0.26 cm^{-1} at the corresponding Raman wavelength of ~2.56 μm (as discussed above, see Fig. 5), the threshold peak intensities at this pump wavelength, for all focusing lens – output coupling combinations, were calculated ($I_{th–1.91μm}$ in Table 1). These are higher than the maximum available peak intensities from the Tm:YLF laser (up to

Optics EXPRESS

~0.54- and ~0.31 GW/cm^2 for the 75- and 100 mm lens respectively). Thus, the DRL in its current configuration is not expected to oscillate under 1.91 µm pumping.

As discussed in the introduction, Tm fiber laser pumps offer the potential to power scale this DRL. In order to achieve this, the pump wavelength that optimizes the wall plug efficiency of the Tm fiber laser / DRL system needs to be identified. By using etalons of different thickness in the cavity, we aim to increase the tunability of the Tm:YLF laser in order to access more wavelengths in the vicinity of 1.9 µm and so identify the longest wavelength at which the DRL can operate efficiently. This information will subsequently determine the long wavelength limit for the Tm fiber pump laser.

4. Conclusions

In conclusion, the feasibility of infrared external cavity diamond Raman lasers operating in the wavelength region of ~2.5 µm has been experimentally demonstrated. The maximum output pulse energy was 1.67 mJ for 4.4 mJ of pump, which yielded a maximum conversion efficiency of 38%. The Raman pulse duration was between 11 and 15 ns (for ~33 ns pump pulse duration) giving peak powers in excess of 100 kW. This represents the first step in identifying the optimum wavelength for Tm fibre laser pumped diamond Raman lasers, paving the way for power scaling in the industrially important ~2.5 µm region, which has considerable implications for the processing of clear plastics.

Funding

Engineering and Physical Sciences Research Council (EPSRC) (EP/P00041X/1); Fraunhofer UK Research Ltd; Royal Academy of Engineering.

Acknowledgments

The authors would like to thank Niall McAlinden for the help he provided with the LabVIEW software for collecting the spectra of Fig. 4. Fraunhofer UK Research Ltd. is acknowledged for acousto-optic modulator and optics loans. Element Six (UK) Ltd. is acknowledged for loan of the 4 mm long diamond.

Disclosures

All data underpinning this publication are openly available from the University of Strathclyde Knowledge Base at https://doi.org/10.15129/d04f42ed-f4cf-4e9c-8944-e763c691b8ed.

References

1. International Organization for Standardization, "Optics and photonics–Spectral bands," in *ISO 20473:2007* (International Organization for Standardization, 2007).
2. M. Ebrahim-Zadeh and I. T. Sorokina, *Mid-Infrared Coherent Sources and Applications* (Springer, 2008).
3. A. K. Majumdar and J. C. Ricklin, *Free-Space Laser Communications. Principles and Advances* (Springer, 2008).
4. R. Klein, *Laser Welding of Plastics: Materials, Processes and Industrial Applications* (Wiley-VCH, 2012).
5. A. Godard, "Infrared (2–12 µm) solid-state laser sources: a review," C. R. Phys. **8**(10), 1100–1128 (2007).
6. S. Vasilyev, I. Moskalev, M. Mirov, V. Smolsky, S. Mirov, and V. Gapontsev, "Recent breakthroughs in solid-state mid-IR saser sechnology," Laser Tech. J. **13**(4), 24–27 (2016).
7. T. T. Basiev, M. N. Basieva, M. E. Doroshenko, V. V. Fedorov, V. V. Osiko, and S. B. Mirov, "Stimulated Raman scattering in mid IR spectral range 2.31–2.75–3.7 µm in $BaWO_4$ crystal under 1.9 and 1.56 µm pumping," Laser Phys. Lett. **3**(1), 17–20 (2006).
8. O. Kuzucu, "Watt-level, mid-infrared output from a $BaWO_4$ external-cavity Raman laser at 2.6 µm," Opt. Lett. **40**(21), 5078–5081 (2015).
9. J. Zhao, X. Zhang, X. Guo, X. Bao, L. Li, and J. Cui, "Diode-pumped actively Q-switched Tm, Ho:$GdVO_4$/$BaWO_4$ intracavity Raman laser at 2533 nm," Opt. Lett. **38**(8), 1206–1208 (2013).
10. Z. Bai, R. J. Williams, O. Kitzler, S. Sarang, D. J. Spence, and R. P. Mildren, "302 W quasi-continuous cascaded diamond Raman laser at 1.5 microns with large brightness enhancement," Opt. Express **26**(16), 19797–19803 (2018).
11. R. Casula, J. P. Penttinen, A. J. Kemp, M. Guina, and J. E. Hastie, "1.4 µm continuous-wave diamond Raman laser," Opt. Express **25**(25), 31377–31383 (2017).

Optics EXPRESS

12. S. D. Jackson, "Towards high-power mid-infrared emission from a fibre laser," Nat. Photonics **6**(7), 423–431 (2012).
13. M. N. Zervas and C. A. Codemard, "High power fiber lasers: a review," IEEE J. Sel. Top. Quantum Electron. **20**(5), 219–241 (2014).
14. D. L. N. Kallepalli, N. R. Desai, and V. R. Soma, "Fabrication and optical characterization of microstructures in poly(methylmethacrylate) and poly(dimethylsiloxane) using femtosecond pulses for photonic and microfluidic applications," Appl. Opt. **49**(13), 2475–2489 (2010).
15. T. T. Basiev, A. A. Sobol, P. G. Zverev, V. V. Osiko, and R. C. Powell, "Comparative spontaneous Raman spectroscopy of crystals for Raman lasers," Appl. Opt. **38**(3), 594–598 (1999).
16. V. G. Savitski, S. Reilly, and A. J. Kemp, "Steady-state Raman gain in diamond as a function of pump wavelength," IEEE J. Quantum Electron. **49**(2), 218–223 (2013).
17. I. Friel, S. L. Geoghegan, D. J. Twitchen, and G. A. Scarsbrook, "Development of high quality single crystal diamond for novel laser applications," in *SPIE Security + Defence* (SPIE, 2010), doi: 10.1117/12.864981.
18. C. A. Klein, "Laser-induced damage to diamond: dielectric breakdown and BHG scaling," in *Laser-Induced Damage in Optical Materials: 1994* (SPIE, 1995), pp. 517–530.
19. S. Reilly, V. G. Savitski, H. Liu, S. Reid, D. Gibson, H. Dhillon, S. O. Robbie, E. Gu, M. D. Dawson, A. Bennett, and A. J. Kemp, "Laser induced damage threshold of CVD-grown single crystal diamond surfaces with various surface finishes," in *Advanced Solid State Lasers* (Optical Society of America, 2015), ATu2A.6.
20. R. P. Mildren, "Intrinsic optical properties of diamond," in *Optical Engineering of Diamond* (Wiley, 2013).
21. A. Sabella, J. A. Piper, and R. P. Mildren, "Diamond Raman laser with continuously tunable output from 3.38 to 3.80 μm," Opt. Lett. **39**(13), 4037–4040 (2014).
22. A. Sincore, J. D. Bradford, J. Cook, L. Shah, and M. C. Richardson, "High average power Thulium-doped silica fiber lasers: review of systems and concepts," IEEE J. Sel. Top. Quantum Electron. **24**(3), 1–8 (2018).
23. R. Paschotta, *Encyclopedia of Laser Physics and Technology* (Wiley-VCH, 2008).
24. K. C. Lee, B. J. Sussman, J. Nunn, V. O. Lorenz, K. Reim, D. Jaksch, I. A. Walmsley, P. Spizzirri, and S. Prawer, "Comparing phonon dephasing lifetimes in diamond using transient coherent ultrafast phonon spectroscopy," Diamond Related Materials **19**(10), 1289–1295 (2010).
25. K. Ishioka, M. Hase, M. Kitajima, and H. Petek, "Coherent optical phonons in diamond," Appl. Phys. Lett. **89**(23), 231916 (2006).
26. D. J. Spence, "Spectral effects of stimulated Raman scattering in crystals," Prog. Quantum Electron. **51**, 1–45 (2017).
27. J. A. Piper and H. M. Pask, "Crystalline Raman lasers," IEEE J. Sel. Top. Quantum Electron. **13**(3), 692–704 (2007).
28. D. C. Parrotta, A. J. Kemp, M. D. Dawson, and J. E. Hastie, "Multiwatt, continuous-wave, tunable diamond Raman laser with intracavity frequency-doubling to the visible region," IEEE J. Sel. Top. Quantum Electron. **19**(4), 1400108 (2013).
29. J. Lin, H. M. Pask, A. J. Lee, and D. J. Spence, "Study of relaxation oscillations in continuous-wave intracavity Raman lasers," Opt. Express **18**(11), 11530–11536 (2010).
30. A. Sabella, D. J. Spence, and R. P. Mildren, "Pump–probe measurements of the Raman gain coefficient in crystals using multi-longitudinal-mode beams," IEEE J. Quantum Electron. **51**(12), 1–8 (2015).